ACS APPLIED MATERIALS & INTERFACES

Letter

www.acsami.org

Selective (Bio)Functionalization of Solid-State Nanopores

Mateu Pla-Roca,[†,‡] Lucio Isa,[†,§] Karthik Kumar,[†,⊥] and Erik Reimhult*[,†,∥]

[†]Department of Materials, ETH Zurich, CH-8093 Zurich, Switzerland

[∥]Department of Nanobiotechnology, University of Natural Resources and Life Sciences Vienna, 1190 Vienna, Austria

Supporting Information

ABSTRACT: We present a method to selectively (bio)-functionalize nanoscale features with the same materials chemistry. It was successfully combined with nanosphere lithography to fabricate and functionalize solid-state nanopores with PEG-brushes, supported lipid membranes, and functional proteins over large areas. The method is inexpensive, can be performed without specialized equipment, and can be applied to both topographic and planar surface modification.

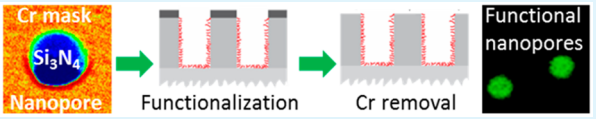

KEYWORDS: *nanosphere lithography, nanopore functionalization, PEG brush, supported lipid bilayer, solid state nanopore*

Engineered nanopores fabricated in free-standing membranes, also called solid-state nanopores, have been used as models to study mimics of DNA translocation through the nuclear pore complex and other biological channels[1,2] and as a tool to study protein−ligand interactions at the single-molecule level.[3] Nanopores are of high interest for ultrafiltration.[4,5] They are considered to have enormous potential for biosensing applications,[4,6] especially to efficiently funnel analytes to optical biosensor elements.[7,8] All applications to complex biomolecular solutions require that the pore is made specifically interacting with the analyte. The top surface should therefore be completely nonfouling and differ in functionality from the pore to maximize sensitivity, prevent clogging, and give high signal-to-noise. Such orthogonal surface (bio)functionalization of topographic 3D structures still requires new methods to be developed.[4,9] Several approaches for selective silanization of the inside and outside of nanopores have been proposed.[10] They are typically complex processes with high failure rates,[4,9,10] relying on phenomena that are difficult to control accurately, such as surface wetting,[11] electrospraying,[12] plasma polymerization,[13] or other methods specific to processing conditions during the anodization of porous alumina.[14] Our work addresses this need for the flexible and robust fabrication of a large range of structures and applications; it extends beyond silanization to physisorbed, self-assembled molecular surface modifications of common use in biosensor surface modification.

Fabrication of nanopore arrays can be accomplished by ion-beam or by nanoscale lithography followed by anisotropic etching. Because of its serial nature, focused ion beam is too slow and expensive to create a large number of pores on multiple biosensor substrates. Metal-mask-assisted etching is a well-established technique to create high aspect ratio nanostructures.[15] The lithographic step can be performed by, e.g., electron-beam or nanoimprint lithography. Nanosphere (NS) lithography is an alternative method to create nanopatterns that has been used to create nanopore arrays in Si_3N_4 and other supports.[8,16,17] It is a low-cost alternative to directly create a nanohole metal mask, but limited to arrays of nanoscale features while arbitrary patterns cannot be produced. The process encompasses the deposition of a metal layer, e.g., Cr, onto a Si_3N_4 surface bearing a monolayer of polystyrene NS deposited randomly[18] or ordered.[19] After removal of the NS, the underlying substrate is anisotropically etched using reactive ion etching through the apertures of the metal mask.[8,16,19] Dissolving the Cr mask leaves a clean substrate perforated with nanopores. We have in previous work demonstrated the regularity of the formed pores, which are routinely obtained with straight and smooth walls and the uniform dimensions given by the colloids used for the original mask.

Specific functionalization of the nanopores is challenging because of the small dimensions and the lack of material contrast between inside and topside. One strategy used for this purpose is the sequential deposition and etching of thin layers of distinct materials on the substrate, such as gold on Si_3N_4 for nanoplasmonic hole sensors.[7,20,21] Responsive polymer brushes were also patterned using radical polymerization in nanopores masked by a Cr film onto which vapor-deposited silane-anchored initiators did not bind.[22] The use of orthogonal binding chemistry, e.g., silanes and thiols, to modify a patterned surface is often referred to as selective molecular assembly patterning (SMAP).[23] This method risks physisorption of molecules on the part of the pattern where they are not supposed to bind.

Alternatively, one part of the surface can first be patterned using a mask.[24] The unmasked pattern can be subsequently functionalized by molecular self-assembly if the mask can be lifted off without disturbing the assembled molecular layer. An example of this approach on the micron scale is the molecular assembly photolithographic lift-off (MAPL) approach.[25] The main advantage of MAPL is that the surface to be patterned in the second step is fully protected during the first functionaliza-

Received: January 6, 2015
Accepted: March 11, 2015
Published: March 11, 2015

DOI: 10.1021/acsami.5b00138
ACS Appl. Mater. Interfaces 2015, 7, 6030−6035

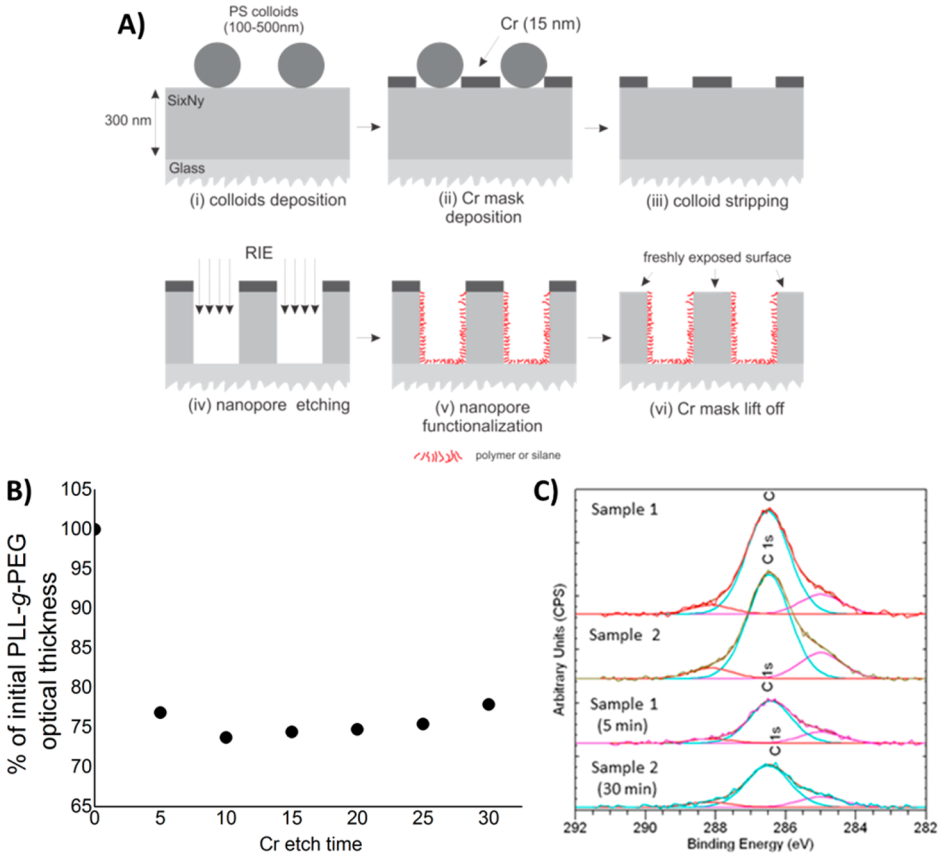

Figure 1. (Ai–vi) Schematic of the process to fabricate and functionalize nanopores in 300 nm Si_3N_4 layers supported on glass. The process results in nanopores coated with protein-resistant PLL-*g*-PEG and a clean Si_3N_4 top surface. (B). TInAS results for the effect of Cr-etching on PLL-*g*-PEG thickness. (C) XPS results for the effect of Cr-etching on PLL-*g*-PEG mass for two samples etched for 5 and 30 min, respectively. Integration of the C 1s peak yields a reduction of 50% after 5 min, which was unchanged after 30 min exposure.

tion step and that the entire surface can have the same surface chemistry. The original MAPL approach has not been successfully downscaled to the nanoscale or applied to weakly self-assembled systems such as lipid membranes. However, Steinem et al. recently extended the concept to hydrophobic silanization of aluminum oxide membranes masked by an Au film.[10] It was shown that the top surface could be rendered hydrophobic to assemble lipid monolayers, whereas the hydrophilic interior of the pores repelled lipid adsorption. In a recent alternative approach, a PDMS stamp masked one side of a nanoporous chip during vapor deposition of an initiator, which resulted in polymerization only in the nanopores and on one side of the chip.[26]

We present a MAPL-related strategy that goes substantially beyond current state-of-the-art. A Cr mask defined by NS lithography is used to control the etching of nanopores (100, 200, and 500 nm in diameter) into a Si_3N_4 membrane. Our objective is to create polymer brushes that suppress nonspecific biomolecular adsorption on either or both the top and inner surfaces of the nanopores, which can have different selective interactions with biological molecules. The brush functionalization of the nanopores is integrated in the lithography process before the removal of the Cr mask. A second type of polymer brush or, for example, a supported lipid bilayer, can be created through self-assembly after mask removal.

Nanopores were generated by NS lithography first in 300 nm thick Si_3N_4 layers deposited on glass, as published previously (Figure 1Ai-iv; see the Supporting Information for AFM and SEM images of substrates).[8,19] A 15 nm thick metallic Cr mask was used in the masking step. The concentration of nanopores on the surface was tuned by adjusting the concentration of NS and the incubation time. Samples with mixed pore sizes were obtained by mixing colloidal dispersions; these were used to compare directly the dependence of the molecular self-assembly on the nanopore size. Functionalization of the pores was performed before the removal of the Cr mask used for the pore etching (Figure 1Av). The Cr mask thus also masks the surface from adsorption of polymer and other contaminations during the nanopore functionalization. Cr mask removal will lift off all molecules adhering to it after the functionalization step and leave a pristine surface for further functionalization, but the etching can also affect the integrity of the polymer adsorbed inside the nanopores. XPS measurements were performed in order to determine the minimal time required to completely remove the Cr mask. After 5 min the Cr layer cannot be observed by optical inspection, but XPS revealed that traces remain on the surface for etching times up to 25 min. The complete removal of all metal traces is important because they affect the wettability and charge of the surface, as well as toxicity when performing biological assays. A 30 min Cr etch was henceforth used to ensure the complete removal of the metal mask (see the Supporting Information for XPS measurements).

Poly-L-lysine-*graft*-poly(ethylene glycol) (PLL-*g*-PEG) and PLL-*g*-PEG-biotin were chosen first for nanopore functionalization.[27,28] The cationic polylysine (PLL) polymer backbone of

DOI: 10.1021/acsami.5b00138
ACS Appl. Mater. Interfaces 2015, 7, 6030–6035

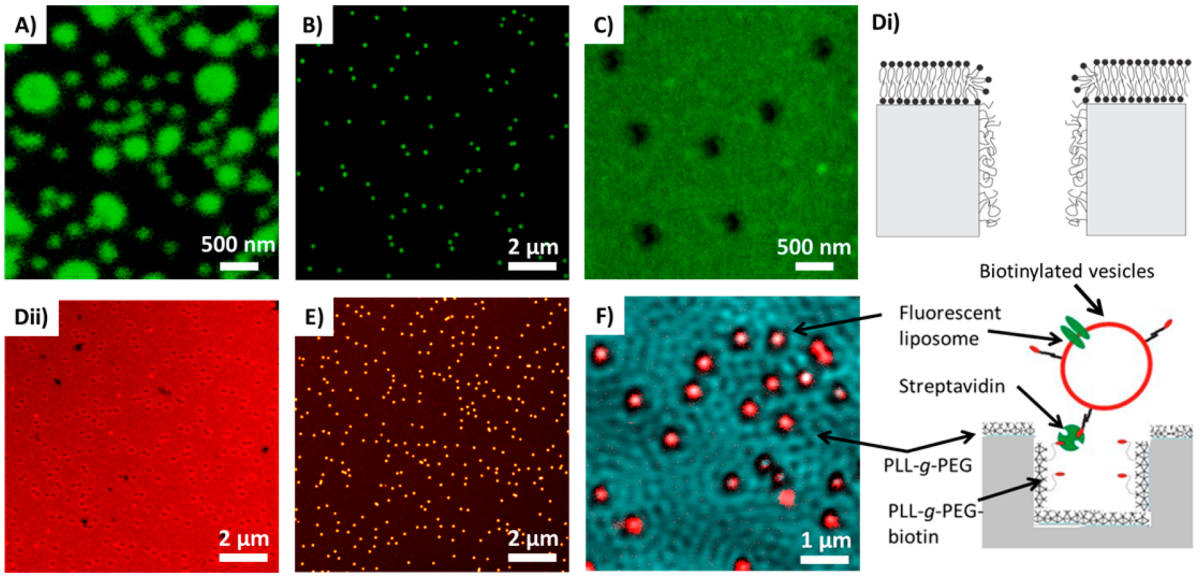

Figure 2. Neutravidin fluorescently labeled with Oregon green (green channel) was selectively bound to surfaces functionalized with a PLL-*g*-PEG-biotin brush on a background functionalized with PEG (dark areas). (A) 100, 200, and 500 nm nanopores functionalized with PLL-*g*-PEG-biotin, backfilled with PLL-*g*-PEG, and exposed to fluorescently-labeled neutravidin. (B) 200 nm nanopores functionalized with PLL-*g*-PEG-biotin and backfilled with PLL-*g*-PEG. C) 200 nm pores functionalized with silane-PEG and the substrate subsequently exposed to PLL-*g*-PEG-biotin. (Di) Schematic of the PEG-functionalized, nonfouling nanopore circumvented by a spontaneously formed supported lipid bilayer. (Dii) The homogeneous red fluorescence demonstrates the formation of a SLB circumventing the 200 nm nanopores functionalized with PLL-*g*-PEG. (E) This selective assembly around the pores contrasts the observation on nonfunctionalized pores where the SLB spreads into the nanopores to produce higher fluorescence from the nanopores.[32] (F) Fluorescence micrograph superimposed on phase contrast image of 200 nm nanopores specifically functionalized with streptavidin capturing liposomes containing a fraction of lipids with biotinylated headgroups; this demonstrates multistep biofunctionalization of the nanopores on a PLL-*g*-PEG nonfouling substrate as well as the possible substitution of neutravidin for streptavidin.

this graft copolymer adsorbs rapidly on freshly UV or plasma activated oxide surfaces due to electrostatic interactions.[27,28] Self-assembly of a well-known nonfouling polymer coating has the advantage over surface-initiated polymerization that it is a one-step, nonchemical process providing a well-characterized polymer brush structure. The optimized graft-copolymer architecture ensures the formation of a dense and stable PEG brush that screens further interactions of the surface with, for example, proteins. The ability of PLL-*g*-PEG to suppress adsorption of many different types of proteins, including serum (albumin), fibrinogen, fibronectin, and cell culture media, liposomes, bacteria, and cells has been amply demonstrated.[29,30] Exposing first the free patterned surface to PLL-*g*-PEG-biotin allows for adding biomolecular functionality on an inert PEGylated background to the inner nanopore walls through the specific bond of biotin to avidin. Via avidin binding, any biotinylated biomolecule, such as antibodies and DNA, can be coupled to the surface.[25,27] Backfilling the entire chip with PLL-*g*-PEG after mask lift off creates a nanoscale biofunctional pattern. A simple assay can be made using fluorescently-labeled neutravidin to image specific nanopore (bio)functionalization. Neutravidin was primarily chosen because of its engineered lower nonspecific interactions compared to native avidin or streptavidin; this is useful if the substrates should be exposed to complex media. Streptavidin was also tested with the same result for controlling specific lipid and protein adsorption as described below.

Investigation of the brush structure inside a nanopore is beyond current experimental capabilities. The stability and integrity of PLL-*g*-PEG adsorbed on Si_3N_4 during exposure to the Cr etching solution was therefore evaluated by means of both transmission interferometric adsorption sensor TInAS[31] and XPS on planar substrates (Figure 1B–C). After 5 min the thickness of the polymer layer as fitted by a one-layer PEG model was reduced by 20%. No further loss of polymer thickness was observed when the etching time was extended stepwise to 30 min. The remaining PLL-*g*-PEG can be removed with a commercial glass or anionic cleaning solution, e.g., Roche COBAS cleaner (Figure 1B). XPS was used to further quantify the changes in terms of polymer film mass by monitoring changes to the C 1s peak area as a function of Cr etch exposure. Again, a rapid loss of polymer mass over the first minutes was observed. Close to 50% of the PLL-*g*-PEG was lost after 5 min. XPS confirmed that 30 min-incubation did not result in additional loss of polymer.

The substantial loss of polymer could reduce the protein repelling property of the PEG brush. It is also possible that the biotin functionality is lost, which would prevent further functionalization. Whether the localized biotin functionality remained or not was tested by binding fluorescently labeled neutravidin to nanopores that had undergone the full process described in Figure 1A. Before exposure to neutravidin the chip was incubated with PLL-*g*-PEG to pacify the top surface and to fill defects on the nanopore walls. Figure 2A shows neutravidin (green fluorescence) selectively captured within PLL-*g*-PEG-biotin functionalized nanopores with diameters of 100, 200, and 500 nm. Nanopore functionalization was accomplished on 100% of the inspected pores (Figure 2B). Comparison of the fluorescence signal of samples etched 5 and 30 min revealed no significant difference; the average intensity signals were 54 ± 8a.u. and 45 ± 5a.u., respectively.

The loss of PLL-*g*-PEG-biotin mass during the etching step could be due to either partial decomposition of the polymer or by reduced surface affinity of the polymer to the surface leading

DOI: 10.1021/acsami.5b00138
ACS Appl. Mater. Interfaces 2015, 7, 6030–6035

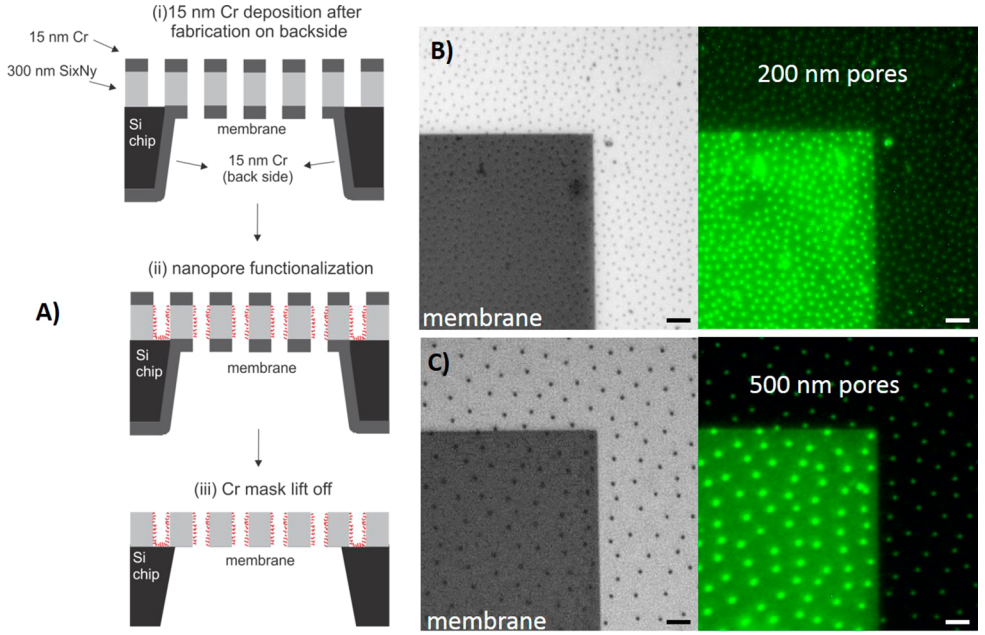

Figure 3. (A) Schematic of the Cr lift-off method to functionalize nanopores on Si_3N_4 membrane sensor chips. (B) 200 and (C) 500 nm PLL-*g*-PEG-biotin-neutravidin functionalized nanoapertures in the Si_3N_4 membrane chip passivated with PLL-*g*-PEG outside the pores. The background signal from the Si_3N_4 membrane around the nanopores is due to scattering (see the Supporting Information, Figure S3). Scale bar 3 μm.

to desorption. The latter is more likely, because the loss occurs through an initial reduction of polymer with no further decomposition upon longer exposure. The affinity of PLL-*g*-PEG is reduced by large changes in pH and the presence of anionic detergents, but after adsorption it is not very sensitive to ionic strength. Desorption could be avoided by covalent binding of the PEG to the substrate using, e.g., silane-PEG to the activated Si_3N_4 surface. Silane-PEG was therefore tested for nanopore functionalization from toluene and the surface backfilled with PLL-*g*-PEG-biotin to create the functional mirror image of the samples functionalized with PLL-*g*-PEG-biotin in the nanopores. Both specific and nonspecific binding of fluorescent neutravidin within the pores can then occur if the coating in the nanopore is damaged by the Cr lift off process, because the PLL-*g*-PEG-biotin can adsorb onto large defects in the silane-PEG coating on the nanopore walls. Figure 2C demonstrates that the silane-PEG coating was not affected by the Cr etching; no neutravidin binding is observed within the nanopores.

Although the silane-PEG approach might be more robust, Figure 2A, B demonstrates that the PLL-*g*-PEG nanopore coating is also sufficient for selective protein capture. PLL-*g*-PEG is easier to handle for surface functionalization because silane-PEG requires water-free conditions. Additionally, samples with pores functionalized with PLL-*g*-PEG could be regenerated for Cr-masking and functionalization by cleaning with, for example, cleaning detergent (Figure 1B). Samples containing 100, 200, and 500 nm pores were reused multiple times with this method without reduction in fluorescence contrast between nanopores and background. Functionalized pore substrates were used for weeks after coating without noticeable differences in results, although PLL-*g*-PEG coated substrates are sensitive to reuse if cleaned in oxidizing environments or by anionic detergents. Silane-PEG substrates could be reused by detergent cleaning with the functionalization intact. Although not directly investigated, the long-term stability even of the PLL-*g*-PEG coating is expected to be a month even if in full media environments as shown, for example, in recent cell studies.[33]

A challenging test is whether the self-assembly of molecules sensitive to the surface composition can proceed after Cr mask removal. The formation of supported lipid bilayers (SLBs) through liposome rupture on the reactivated Si_3N_4 surface is very sensitive to minute amounts of surface contaminations. Cr arrests the rupture of adsorbed liposomes to SLBs.[34] Figure 2D shows a substrate comprising 200 nm PLL-*g*-PEG functionalized nanopores exposed to phosphocholine liposomes after the Cr mask was removed. Adsorption of the liposomes led to formation of a continuous and fluid SLB that does not enter the pores (see also the Supporting Information, Video 1, where the adsorption and rupture of individual liposomes was monitored). The uniform fluorescence intensity demonstrates the formation of a SLB through vesicle fusion. Fluorescence recovery after bleaching further demonstrated that SLB was fluid with a mobile fraction of ~85−95% and a diffusion coefficient calculated to be ~1.5 $\mu m^2/s$ using the method of Soumpasis[35] (see the Supporting Information, Video 2). The nanopore surface coating with PLL-*g*-PEG prevents membrane surface attachment and spreading into the nanopores, which otherwise would take place for pores of this size.[32] The same result was observed when SLB formation experiments were performed on silane-PEG functionalizated nanopores. Figure 2E shows how nonfunctionalized pores have higher fluorescence than the background due to the higher projected amount of lipids within them.[32] As expected, reduced liposome adsorption and absence of SLB formation was observed if the Cr etching time was reduced to 5 min. Finally, in Figure 2F, we demonstrate that the PLL-*g*-PEG-biotin nanopore functionalization in a PLL-*g*-PEG passivated chip is not limited to one-step specific capture of neutravidin. Streptavidin was used to further capture liposomes with a fraction of lipids with biotinylated headgroups. A high yield of liposome functionalized pores was achieved with no indication of streptavidin or liposomes adsorbing nonspecifically to the PEGylated surface.

DOI: 10.1021/acsami.5b00138
ACS Appl. Mater. Interfaces 2015, 7, 6030−6035

The selective nanopore functionalization process was also applied to chips with free-standing Si_3N_4 membranes containing nanopores; these chips were developed for membrane sensing by Porenix AB (Sweden). Large area arrays of quasi-hexagonally ordered nanopores were created on the chips using SALI NS lithography,[19] which leaves a 15 nm Cr mask on the remaining surface that can be used as lift off mask for the selective nanoaperture functionalization (Figure 3). An additional layer of Cr was deposited on the back of the Si_3N_4 membrane to avoid PLL-*g*-PEG-biotin adsorption to this side. Figures 3B, C show chips with, respectively, 200 and 500 nm nanopores. The fluorescence images show the samples after functionalization with PLL-*g*-PEG-biotin within the nanopores, passivation with PLL-*g*-PEG after Cr lift-off for 30 min and exposure to fluorescently-labeled neutravidin. The successful passivation outside of the pores is demonstrated by the lack of top-side fluorescence. Scattering from the pores produced the high window background signal, which was shown by the lack of fluorescence on the Si_3N_4 areas surrounding the Si_3N_4 window (see Supporting Information).

We have demonstrated a convenient method to (bio)-functionalize selective nanoscale features with the same materials chemistry using a metal mask lift-off strategy. The method was successfully combined with inexpensive NS lithography. The retained nonfouling, specific biomolecule capture in nanopores and self-assembly of lipid membranes at the pores allowed us to demonstrate potential application to both affinity and membrane biosensing with fluorescence or electrochemical readout.

■ ASSOCIATED CONTENT

Supporting Information

Detailed experimental descriptions and additional figures and videos are available. This material is available free of charge via the Internet at http://pubs.acs.org.

■ AUTHOR INFORMATION

Corresponding Author

*E-mail: erik.reimhult@boku.ac.at.

Present Addresses

[‡]M.P.-R. is currently at the Platform of Nanotechnology, Institute for Bioengineering of Catalonia, Parc Científic de Barcelona, 08029, Barcelona, Spain

[§]L.I. is currently at the Laboratory for Interfaces, Soft matter and Assembly, ETH Zurich, CH-8093 Zurich, Switzerland

[⊥]K.K. is currently at the Research and Enterprise Division, Ministry of Trade and Industry, Singapore 179434

Author Contributions

The manuscript was written through contributions of all authors. M.P.R. performed the majority of experiments and analysis. All authors have given approval to the final version of the manuscript.

Notes

The authors declare no competing financial interest.

■ ACKNOWLEDGMENTS

We acknowledge the FIRST Center for Micro- and Nanoscience and the Light Microscopy Centre (ETH Zurich) for facilities and support. EU-FP7-NMP-ASMENA (Grant no. CF-FP 214666-2) is acknowledged for financial support. Porenix AB and Adrienne Nelson are acknowledged for the SALI-patterned membrane chips; Antonella Rossi and Stefan Zürcher for the XPS measurements; and Professor Marcus Textor for discussions and support.

■ REFERENCES

(1) Kowalczyk, S. W.; Kapinos, L.; Blosser, T. R.; Magalhaes, T.; van Nies, P.; Lim, R. Y. H.; Dekker, C. Single-Molecule Transport across an Individual Biomimetic Nuclear Pore Complex. *Nat. Nanotechnol.* **2011**, *6*, 433−438.

(2) Venkatesan, B. M.; Bashir, R. Nanopore Sensors for Nucleic Acid Analysis. *Nat. Nanotechnol.* **2011**, *6*, 615−624.

(3) Yusko, E. C.; Johnson, J. M.; Majd, S.; Prangkio, P.; Rollings, R. C.; Li, J.; Yang, J.; Mayer, M. Controlling Protein Translocation through Nanopores with Bio-Inspired Fluid Walls. *Nat. Nanotechnol.* **2011**, *6*, 253−260.

(4) Mey, I.; Steinem, C.; Janshoff, A. Biomimetic Functionalization of Porous Substrates: Towards Model Systems for Cellular Membranes. *J. Mater. Chem.* **2012**, *22*, 19348−19356.

(5) Lee, S. B.; Mitchell, D. T.; Trofin, L.; Nevanen, T. K.; Soderlund, H.; Martin, C. R. Antibody-Based Bio-Nanotube Membranes for Enantiomeric Drug Separations. *Science* **2002**, *296*, 2198−2200.

(6) de la Escosura-Muniz, A.; Merkoci, A. Nanochannels Preparation and Application in Biosensing. *ACS Nano* **2012**, *6*, 7556−7583.

(7) Jonsson, M. P.; Dahlin, A. B.; Feuz, L.; Petronis, S.; Hook, F. Locally Functionalized Short-Range Ordered Nanoplasmonic Pores for Bioanalytical Sensing. *Anal. Chem.* **2010**, *82*, 2087−2094.

(8) Reimhult, E.; Kumar, K.; Knoll, W. Fabrication of Nanoporous Silicon Nitride and Silicon Oxide Films of Controlled Size and Porosity for Combined Electrochemical and Waveguide Measurements. *Nanotechnology* **2007**, *18*, 275303.

(9) Busby, M.; Kerschbaumer, H.; Calzaferri, G.; De Cola, L. Orthogonally Bifunctional Fluorescent Zeolite-L Microcrystals. *Adv. Mater.* **2008**, *20*, 1614−1618.

(10) Lazzara, T. D.; Kliesch, T.-T.; Janshoff, A.; Steinem, C. Orthogonal Functionalization of Nanoporous Substrates: Control of 3d Surface Functionality. *ACS Appl. Mater. Interfaces* **2011**, *3*, 1068−1076.

(11) Kilian, K. A.; Bocking, T.; Gaus, K.; Gooding, J. J. Introducing Distinctly Different Chemical Functionalities onto the Internal and External Surfaces of Mesoporous Materials. *Angew. Chem., Int. Ed. Engl.* **2008**, *47*, 2697−2699.

(12) Jee, S. E.; Lee, P. S.; Yoon, B. J.; Jeong, S. H.; Lee, K. H. Fabrication of Microstructures by Wet Etching of Anodic Aluminum Oxide Substrates. *Chem. Mater.* **2005**, *17*, 4049−4052.

(13) Brevnov, D. A.; Barela, M. J.; Brooks, M. J.; Lopez, G. P.; Atanassov, P. B. Fabrication of Anisotropic Super Hydrophobic/Hydrophilic Nanoporous Membranes by Plasma Polymerization of C4f8 on Anodic Aluminum Oxide. *J. Electrochem. Soc.* **2004**, *151*, B484−B489.

(14) Mutalib Md Jani, A.; Anglin, E. J.; McInnes, S. J. P.; Losic, D.; Shapter, J. G.; Voelcker, N. H. Nanoporous Anodic Aluminium Oxide Membranes with Layered Surface Chemistry. *Chem. Commun. (Cambridge, U. K.)* **2009**, 3062−4.

(15) Li, X. L. Metal Assisted Chemical Etching for High Aspect Ratio Nanostructures: A Review of Characteristics and Applications in Photovoltaics. *Curr. Opin. Solid State Mater. Sci.* **2012**, *16*, 71−81.

(16) Fredriksson, H.; Alaverdyan, Y.; Dmitriev, A.; Langhammer, C.; Sutherland, D. S.; Zaech, M.; Kasemo, B. Hole-Mask Colloidal Lithography. *Adv. Mater. (Weinheim, Ger.)* **2007**, *19*, 4297−4302.

(17) Yang, S. M.; Jang, S. G.; Choi, D. G.; Kim, S.; Yu, H. K. Nanomachining by Colloidal Lithography. *Small* **2006**, *2*, 458−475.

(18) Hanarp, P.; Sutherland, D. S.; Gold, J.; Kasemo, B. Control of Nanoparticle Film Structure for Colloidal Lithography. *Colloids Surf., A* **2003**, *214*, 23−36.

(19) Isa, L.; Kumar, K.; Muller, M.; Grolig, J.; Textor, M.; Reimhult, E. Particle Lithography from Colloidal Self-Assembly at Liquid-Liquid Interfaces. *ACS Nano* **2010**, *4*, 5665−5670.

(20) Mey, I.; Stephan, M.; Schmitt, E. K.; Muller, M. M.; Ben Amar, M.; Steinem, C.; Janshoff, A. Local Membrane Mechanics of Pore-Spanning Bilayers. *J. Am. Chem. Soc.* **2009**, *131*, 7031−7039.

DOI: 10.1021/acsami.5b00138
ACS Appl. Mater. Interfaces 2015, 7, 6030−6035

(21) Hennesthal, C.; Steinem, C. Pore-Spanning Lipid Bilayers Visualized by Scanning Force Microscopy. *J. Am. Chem. Soc.* **2000**, *122*, 8085−8086.
(22) de Groot, G. W.; Santonicola, M. G.; Sugihara, K.; Zambelli, T.; Reimhult, E.; Voros, J.; Vancso, G. J. Switching Transport through Nanopores with Ph-Responsive Polymer Brushes for Controlled Ion Permeability. *ACS Appl. Mater. Interfaces* **2013**, *5*, 1400−1407.
(23) Lussi, J. W.; Michel, R.; Reviakine, I.; Falconnet, D.; Goessl, A.; Csucs, G.; Hubbell, J. A.; Textor, M. A Novel Generic Platform for Chemical Patterning of Surfaces. *Prog. Surf. Sci.* **2004**, *76*, 55−69.
(24) Falconnet, D.; Koenig, A.; Assi, T.; Textor, M. A Combined Photolithographic and Molecular-Assembly Approach to Produce Functional Micropatterns for Applications in the Biosciences. *Adv. Funct. Mater.* **2004**, *14*, 749−756.
(25) Falconnet, D.; Csucs, G.; Grandin, H. M.; Textor, M. Surface Engineering Approaches to Micropattern Surfaces for Cell-Based Assays. *Biomaterials* **2006**, *27*, 3044−3063.
(26) de Groot, G. W.; Demarche, S.; Santonicola, M. G.; Tiefenauer, L.; Vancso, G. J. Smart Polymer Brush Nanostructures Guide the Self-Assembly of Pore-Spanning Lipid Bilayers with Integrated Membrane Proteins. *Nanoscale* **2014**, *6*, 2228−2237.
(27) Huang, N. P.; Voros, J.; De Paul, S. M.; Textor, M.; Spencer, N. D. Biotin-Derivatized Poly(L-Lysine)-G-Poly(Ethylene Glycol): A Novel Polymeric Interface for Bioaffinity Sensing. *Langmuir* **2002**, *18*, 220−230.
(28) Kenausis, G. L.; Voros, J.; Elbert, D. L.; Huang, N. P.; Hofer, R.; Ruiz-Taylor, L.; Textor, M.; Hubbell, J. A.; Spencer, N. D. Poly(L-Lysine)-G-Poly(Ethylene Glycol) Layers on Metal Oxide Surfaces: Attachment Mechanism and Effects of Polymer Architecture on Resistance to Protein Adsorption. *J. Phys. Chem. B* **2000**, *104*, 3298−3309.
(29) Harris, L. G.; Tosatti, S.; Wieland, M.; Textor, M.; Richards, R. G. Staphylococcus Aureus Adhesion to Titanium Oxide Surfaces Coated with Non-Functionalized and Peptide-Functionalized Poly(L-Lysine)-Grafted-Poly(Ethylene Glycol) Copolymers. *Biomaterials* **2004**, *25*, 4135−4148.
(30) Huang, N. P.; Michel, R.; Voros, J.; Textor, M.; Hofer, R.; Rossi, A.; Elbert, D. L.; Hubbell, J. A.; Spencer, N. D. Poly(L-Lysine)-G-Poly(Ethylene Glycol) Layers on Metal Oxide Surfaces: Surface-Analytical Characterization and Resistance to Serum and Fibrinogen Adsorption. *Langmuir* **2001**, *17*, 489−498.
(31) Heuberger, M.; Balmer, T. E. The Transmission Interferometric Adsorption Sensor. *J. Phys. D: Appl. Phys.* **2007**, *40*, 7245−7254.
(32) Kumar, K.; Isa, L.; Egner, A.; Schmidt, R.; Textor, M.; Reimhult, E. Formation of Nanopore-Spanning Lipid Bilayers through Liposome Fusion. *Langmuir* **2011**, *27*, 10920−10928.
(33) Hardelauf, H.; Waide, S.; Sisnaiske, J.; Jacob, P.; Hausherr, V.; Schobel, N.; Janasek, D.; van Thriel, C.; West, J. Micropatterning Neuronal Networks. *Analyst* **2014**, *139*, 3256−3264.
(34) Groves, J. T.; Ulman, N.; Boxer, S. G. Micropatterning Fluid Lipid Bilayers on Solid Supports. *Science* **1997**, *275*, 651−653.
(35) Soumpasis, D. M. Theoretical-Analysis of Fluorescence Photobleaching Recovery Experiments. *Biophys. J.* **1983**, *41*, 95−97.

DOI: 10.1021/acsami.5b00138
ACS Appl. Mater. Interfaces 2015, 7, 6030−6035